Available online at www.sciencedirect.com
ScienceDirect
Ceramics International 36 (2010) 781–788
CERAMICS INTERNATIONAL
www.elsevier.com/locate/ceramint

Zirconia toughening of mullite–zirconia–zircon composites obtained by direct sintering

N.M. Rendtorff [a,b,*], L.B. Garrido [a], E.F. Aglietti [a,b]

[a] Centro de Tecnología de Recursos Minerales y Cerámica (CETMIC): (CIC-CONICET-CCT La Plata), Camino Centenario y 506, C.C.49 (B1897ZCA) M.B. Gonnet, Buenos Aires, Argentina
[b] Facultad de Ciencias Exactas - Universidad Nacional de La Plata, UNLP, Argentina

Received 10 July 2009; received in revised form 6 August 2009; accepted 10 October 2009
Available online 13 November 2009

Abstract

Although multi-phase ceramic materials were always used, nowadays composite materials have an important industrial and technological role, because they enlarge the design capability of the manufacturer in properties and behaviors.

Some mullite–zirconia–zircon composites were recently processed and characterized which presented satisfactory properties for structural applications under severe chemical and thermomechanical conditions. The objective of the present work is to study the influence of the starting composition in the mechanical and fracture properties of mullite–zirconia–zircon composites, with different microstructures, obtained by direct sintering of binary mixtures of electrofused mullite–zirconia (MZ) and micronized zircon. The materials were consolidated by slip casting of concentrated aqueous suspensions in plaster molds from a wide range of powder compositions (between 15–85 wt% and 85–15 wt% of the two raw materials used).

Flexural strength (σ_f), dynamic elastic modulus (E), toughness (K_{IC}) and fracture surface energy (γ_{NBT}) were evaluated. The results were explained by microstructure and the XRD-Rietveld analysis.

At low proportion, the zircon was thermally dissociated. The ZrO_2 was a product of this reaction and also influenced the mechanical and fracture properties of these materials through several combined mechanisms, principally as a result of the development of microcracks due to the volume change of the zirconia grains caused by the martensitic transformation during the cooling of these composites from sintering temperature.

Composites prepared with higher MZ in the starting powders showed a higher fracture toughness and initiation energy. Microstructure consisting of mullite as a continuous predominant phase in which zircon and zirconia grains were distributed showed better mechanical and fracture properties.

Keywords: C. Mechanical properties; D. Mullite; ZrO_2; Zircon; Toughening; Fracture properties

1. Introduction

Composite materials have an important industrial and technological role. The designing capability of the manufacturer in properties and behaviors is enhanced by combining two or more different materials. However the final properties will not always be between the pure material ones. Once the constituent phases and the processing conditions are chosen the phase's proportion becomes one of the most important processing variables.

Zircon ($ZrSiO_4$) is a good refractory material because it does not undergo any structural transformation until its dissociation at about 1450–1700 °C, depends on the impurities. It exhibits many attractive properties such as excellent chemical stability, a very low thermal expansion coefficient (4.1×10^{-6} °C^{-1}) from room temperature to 1400 °C and low heat conductivity coefficient (5.1 W/m °C at room temperature and 3.5 W/m °C at 1000 °C). Sintered zircon with high purity can retain its bending strength up to temperatures of 1200 °C and 1400 °C [1]. These properties make zircon a useful structural ceramic. These materials are widely utilized in the glass industries [2–4]. The presence of impurities decreases the dissociation and use temperatures.

* Corresponding author at: Centro de Tecnología de Recursos Minerales y Cerámica (CETMIC): (CIC-CONICET-CCT La Plata), Camino Centenario y 506, C.C.49 (B1897ZCA) M.B. Gonnet, Buenos Aires, Argentina.
Tel.: +54 2214840247; fax: +54 2214710075.
E-mail address: rendtorff@cetmic.unlp.edu.ar (N.M. Rendtorff).

0272-8842/$36.00
doi:10.1016/j.ceramint.2009.11.010

The mullite ceramics have had and will continue to have a significant role in the development of traditional and advanced ceramics [5–7]. Mullite is the only stable crystalline phase in the aluminosilicate system, under normal atmospheric pressure at room through elevated temperatures [6]. Its chemical composition ranges from $3Al_2O_3$–$2SiO_2$ to approximately $2Al_2O_3$–SiO_2. It has received significant attention during the last decades as a potential structural material for high temperature applications [7].

Zircon based ceramics have been processed in several ways, for example by room temperature pressing, hot pressing, sol–gel and slip casting [8–11]. Zircon materials sintered in the range between 1500 °C and 1650 °C achieved densities over the 99% of the theoretical depending on the processing route. There are several studies of composites with zircon as the principal phase [12–16]. And more than a few studies of composites with mullite [5–7]. Zircon–mullite material obtained by a reaction sintering and direct sintering had been the objective of resent studies [14,16]. Due to of the dissociation of zircon the material was actually a zircon–mullite–zirconia material with low proportions of zirconia ($\leq$12%). Although zircon and mullite are different from the chemical and crystallographic point of view, their mechanical properties are similar.

The extensive zirconia composite uses are due to the fact that the zirconia dispersion in the ceramic matrix improves the thermomechanical properties, leading to toughness by transformation and microcracking. Besides, microcracks due to the martensitic transformation may cause the dissipation or absorption of strain energy by crack spreading. For this reason these composites are likely to have good thermal shock resistance [17].

Particularly in refractories, mullite and zirconia are both phases resulting from the use of zircon in high alumina content compositions. Such refractories containing mullite–zirconia as main phases can be prepared by several routes including sintering electrofused mullite–zirconia (MZ) grains which are nowadays available in the market [17–19,4,20].

Recently some mullite–zirconia–zircon materials were prepared and characterized [21]. In this work the influence of the different phase contents and microstructural configurations was examined and correlated with a textural, structural, mechanical and fracture properties.

2. Experimental

2.1. Materials

The materials studied in the present work were partially characterized, particularly in terms of their thermal shock behavior [15,21]. Two commercial raw materials were used to obtain the three phase composite material: for the first two principal phases a commercial powder of mullite–zirconia (MZ) (MUZR, ELFUSA LT, Brazil) elaborated from the fusion of raw materials of high purity in electrical arc furnaces was used. Table 1 shows the chemical analysis of this electrofused material given by the manufacturer (www.elfusa.com.br). Fusion point: 1850 °C; apparent specific mass (NBR8592-1995): 3.71 g/cm^3; apparent porosity (NBR8592-1995): 3.0%; real density: 3.74 g/cm^3; reversible linear expansion (1400 °C): 0.68%. The $<$10 μm fraction (obtained by sedimentation) was milled by attrition up to have a fine powder (mean diameter, D_{50} = 5 μm). This material is composed of mullite and m-ZrO_2 as major crystalline phases. The actual composition was described in a previous work [20].

Zircon, the third principal phase, was introduced as zirconium silicate (Z) (Mahlwerke Kreutz, Mikron, Germany), with ZrO_2 = 64–65.5 wt%, SiO_2 = 33–34 wt%, $Fe_2O_3 \leq 0.10$ wt% and $TiO_2 \leq 0.15$ wt% and D_{50} = 1.5 μm. Specific gravity of 4.6 g/cm^3, melting point of 2200 °C and hardness (Mohs) of 7.5.

MZZ composites were prepared from MZ grains and zircon mixtures containing 15%, 25%, 35%, 45%, 55%, 65%, 75% and 85% (in weight basis) of zircon and were called MZZ15, MZZ25, MZZ35, MZZ45, MZZ55, MZZ65, MZZ75 and MZZ85 respectively.

Concentrated 80 wt% suspensions at pH 9.1–9.2 were prepared by adding the powder to aqueous solutions with 0.3% of dispersant (Dolapix CE64, Zschimmers and Schwartz) and NH_4OH. After mixing, the suspensions were ultrasonicated for 20 min. This was slip cast into prismatic bars of 7.5 mm × 7.5 mm × 50 mm. Samples were sintered at a heating rate of 5 °C/min up to 1600 °C for 2 h and then cooled to room temperature at 5 °C/min.

2.2. Characterization techniques

Density and open porosity of sintered samples were determined by the water absorption method. Crystalline phases

Table 1
Textural properties and volume composition (V_i) of the studied materials.

Material	Apparent density (g/cm^3)	Open porosity (%)	Final crystalline phases		
			Mullite (vol%)	Zirconia (total) (vol%)	Zircon (vol%)
MZZ15	3.4	3.7	61	38	1
MZZ25	3.5	4.3	61	39	0
MZZ35	3.6	3.6	49	32	19
MZZ45	3.7	5.6	45	28	27
MZZ55	3.9	5.0	37	20	43
MZZ65	3.9	4.0	29	12	59
MZZ75	4.0	3.0	21	9	70
MZZ85	4.1	2.0	14	5	81

formed were analyzed by X-ray diffraction (XRD) (Philips 3020 equipment with Cu-Kα radiation in Ni filter at 40 kV–20 mA). The Rietveld method [22,23], a quantitative analysis, was carried out to characterize the present crystalline phases in the materials. The XRD patterns were analyzed with the program FullProf, which is a multipurpose profile-fitting program, including Rietveld refinement [24].

Microstructural examination was conducted with a scanning electron microscope SEM (Quanta 200 MK2 Series de FEI) after polishing the surface to 0.25 μm diamond paste.

Flexural strength (σ_f) was measured on the bars with rectangular section using the 3-point bending test with 40 mm of span and a displacement rate of 2.5 mm/min was employed (universal testing machine INSTRON 4483).

The dynamic elastic modulus E of the composites was measured by the excitation technique with a GrindoSonic, MK5 "Industrial" Model. A theoretical estimation of the elastic modulus (E_{teo}) was made; this was defined by the following expression:

$$E_{teo} = \sum (E_i \cdot V_i) \quad (1)$$

where E_i and V_i are the elastic modulus and the volume fraction of each crystalline phase, respectively. The values for each phase elastic modulus were (244 GPa, 204 GPa and 200 GPa for zircon, mullite and m-ZrO_2, respectively). The volume fraction was estimated from the theoretical densities and the weight fractions evaluated by the Rietveld method.

The fracture toughness (K_{IC}) and the fracture initiation energy (γ_{NBT}) were evaluated by the single edge notched beam test (NBT) [25,26] using a 3-point bend test in a universal testing machine (universal testing machine INSTRON 4483). Samples of dimensions (7.5 mm × 7.5 mm × 50 mm) were notched with diamond saw of 0.3 mm thickness, with depth between 0.3 mm and 2.5 mm. The 3-point test was carried out at room temperature with a rate displacement of 0.1 mm/min. In this method K_{IC} (in MPa $m^{1/2}$) is given by:

$$K_{IC} = \frac{3QLC^{1/2}}{2WD^2}\left[A_0 + A_1\left(\frac{C}{D}\right) + A_2\left(\frac{C}{D}\right)^2 + A_3\left(\frac{C}{D}\right)^3 + A_4\left(\frac{C}{D}\right)^4\right]$$

where Q is the load applied to the notched bar, L is the span, C is the depth of the notch, D is the thickness of the specimen, W is the width of the specimen, and A_0, A_1, A_2, A_3 and A_4 are functions of the ratio (L/D) described in [19,4].

Finally, the calculated values of K_{IC}, together with the dynamic modulus of elasticity (E), were used to estimate the fracture energy for the area created by the crack propagation (γ_{NBT}) evaluated by the NBT test, using the following equations [25,26]:

$$K_{IC} = \sqrt{2\gamma_{NBT}E} \quad (3)$$

where γ_{NBT} can be expressed as follows:

$$\gamma_{NBT} = \frac{K_{IC}^2}{2E} \quad (4)$$

3. Results and discussion

3.1. Porosity and composition

A progressive change of microstructure is intended with the gradual change in the initial raw materials proportions. Direct sintering is an easy route for obtaining ceramic composites, no important chemical reactions are expected and densification would be only achieved due to the high temperature treatment if the consolidating particle packing is suitably efficient. If the thermal treatment is sufficiently short no important grain growth will be anticipated and the microstructure obtained will be of the same order of the grain size of the raw materials.

As mentioned before, the objective of the present work is to correlate the initial composition with the mechanical and fracture properties of this family of composites. As the composition range is wide, several microstructure configurations will be achieved

The porosity of the materials are shown in Table 1, all the materials processed showed a low total porosity. All the composite material showed a relatively high density (≈90%) due to the processing route (slip casting). Some close porosity existed and glassy phase is expected to occur at the grain boundaries. The sintering parameters used showed that the microstructures of all the materials studied will be of the same order. Hence the results from changes in the mechanical and fracture properties are dependent only on the phase composition and microstructure configuration.

3.2. Crystalline phases present

Diffraction patterns of the materials are shown in Fig. 1. The major phases in the composite were mullite, m-ZrO_2 (monoclinic zirconia) and zircon labeled with M, B and Z respectively. The gradual change in the phase contents is clearly shown in Fig. 2 where the patterns of the composites are

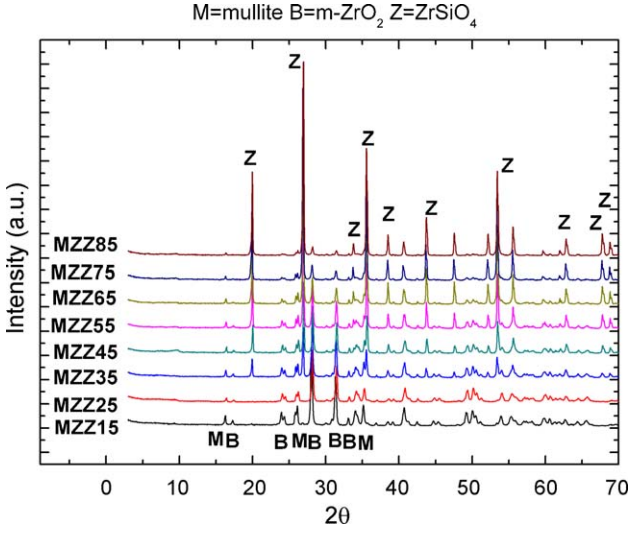

Fig. 1. Diffraction patterns of the studied materials. (For interpretation of the references to color in this artwork, the reader is referred to the web version of the article.)

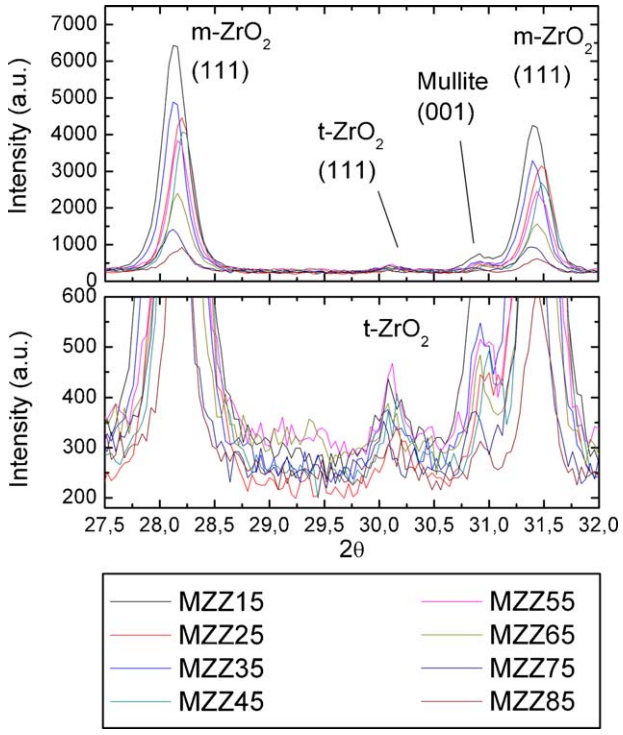

Fig. 2. Superposed diffraction patterns of the studied materials (detail). (For interpretation of the references to color in this artwork, the reader is referred to the web version of the article.)

superposed; the lower pattern corresponds to the MZZ85 composite while the higher pattern corresponds to the MZZ15 composite. Small reflections of t-ZrO_2 can be observed in Fig. 2, which is a detail of the previous XRD pattern.

Initial and final compositions of the composites studied are shown in Fig. 3, evaluated from the compositions of the raw materials employed (full lines) and the phase composition evaluated by the Rietveld method after sintering (dash lines). Mullite contents remain constant after the processing of the composites.

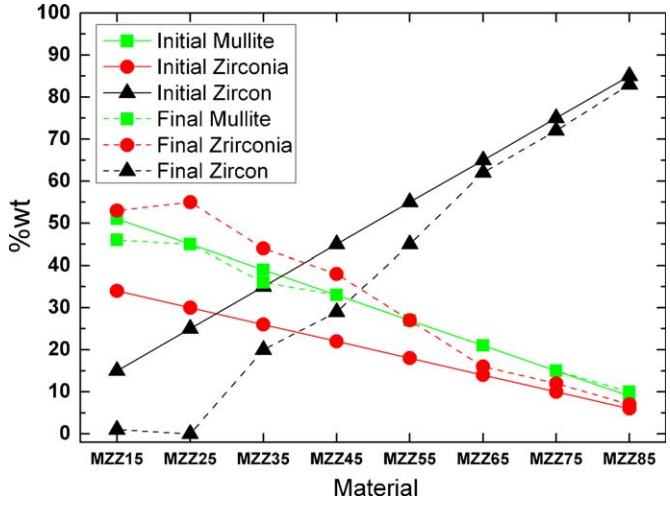

Fig. 3. Initial and final composition of the materials studied. (For interpretation of the references to color in this artwork, the reader is referred to the web version of the article.)

Table 1 also shows the final composition expressed as volume percentage estimated by Eq. (5).

$$V_i = \frac{m_i/d_i}{\sum m_i/d_i} \times 100 \quad (5)$$

where m_i is the mass fraction evaluated by the Rietveld method, and d_i is the theoretical density of each phase. Due to the low density of mullite compared to the other phases (3.13 g/cm^3 for mullite, 4.56 g/cm^3 for zircon and 5.89 for zirconia) its volume content was higher than that in the weight composition and reached up to 60 vol%.

The temperature at which thermal dissociation of the zircon starts depends on the presence of impurities and other phases [27]. In the composites with a low zircon content (15–25 wt%) no zircon diffractions are detected (XRD), hence it has decomposed completely. On the other hand, in the rest of the composites the thermal dissociation is partial; moreover when the zircon proportion is over 55 wt% the dissociation is less than 5%. It can be assumed that the SiO_2, coming from the decomposition reaction, is in the glassy phase of the material [27]. Fig. 4 shows the fraction of zircon dissociated as a function of the amount of mullite–zirconia raw material present when the composite was formulated. This particular behavior may be explained by the fact that the zircon dissociation occurs in the grain boundaries of zircon with a second phase [16,27] (in this case mullite or zirconia) and in the cases where the zircon grain are surrounded by other phases, during the thermal treatment its dissociations occurs completely.

Zirconia undergoes martensitic transformation from monoclinic to tetragonal phase at around 1100 °C in a heating (semi-cycle) step and the inverse transformation during cooling occurs around 900 °C, but it has been stated that if the grain is smaller than a critical size the tetragonal phase is retained. So the small presence of the t-ZrO_2 (less than 1 wt% by Rietveld analysis) indicated the existence of zirconia particles smaller than its critical size is negligible, consequently the inverse transformation occurred almost completely. This transformations is accompanied by a volume change, therefore micro-

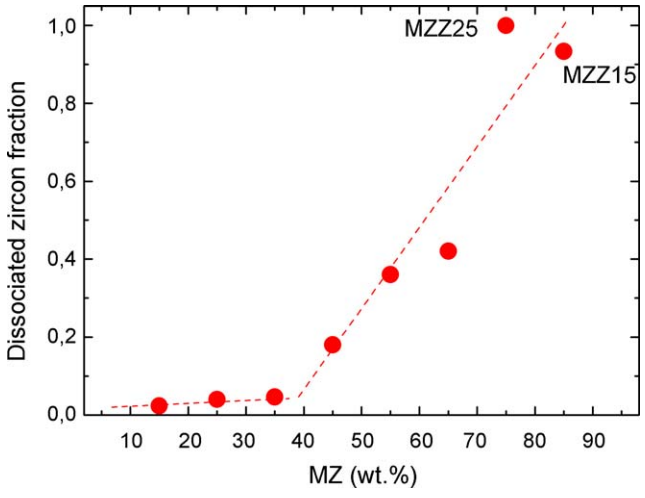

Fig. 4. Amount of dissociated zircon as a function of the MZ content.

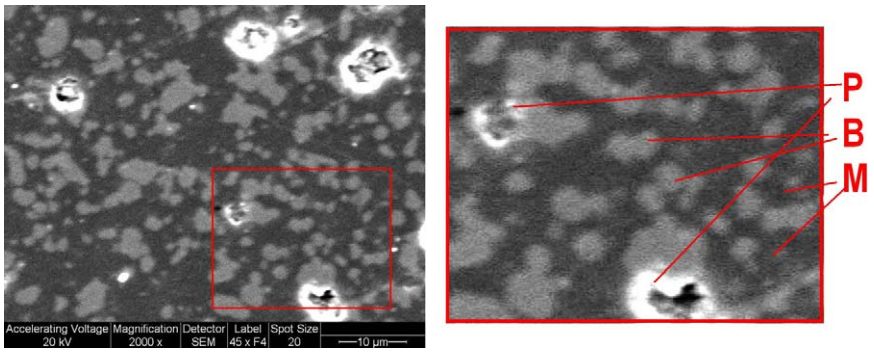

Fig. 5. SEM micrograph of the MZZ25 material. Example of the A type microstructure.

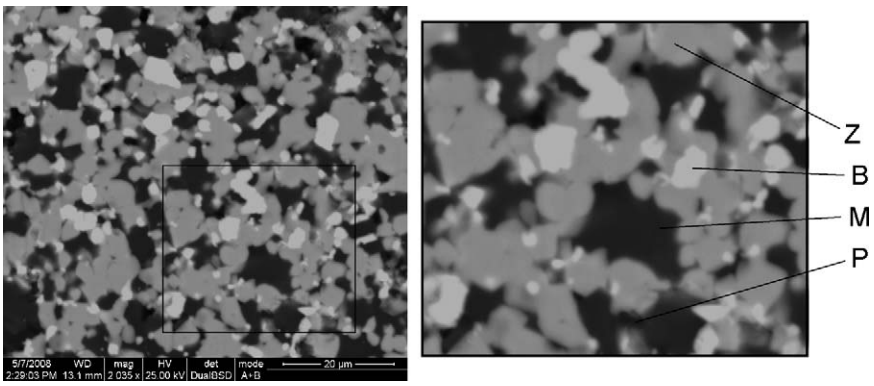

Fig. 6. SEM micrograph of the MZZ55 material. Example of the B type microstructure.

cracks develop around the zirconia grains dispersed in the ceramic matrix. A second mechanism of microcrack development is the local thermal dilatation mismatch between the different ceramic phases present in the composite.

3.3. Microstructure

Figs. 5–7 show the SEM micrographs of the MZZ25, MZZ55, MZZ75 materials respectively (2000× and 4000×).

All the samples presented a dense microstructure with low residual porosity (*P*). There is no a preferential direction or orientation of the grains in the microstructures of these materials. The images demonstrate that high sintering was achieved for all the composites. Different crystalline phases in all the samples were observed and characterized by EDAX. Dark gray grains of mullite (M), middle gray grains of zircon (Z) and zirconia white grains can be observed (B) which are from the MZ raw material and others from the thermal decomposition of the zircon.

The initial mean diameter of the starting powders was below 5 μm in all the cases hence as the grain diameters observed where slightly bigger indicating that some grain growth occurs during sintering. In Fig. 5, no zircon grains were detected (Zr:Si ratio was high in the EDAX examination of the lighter grains), concordant with the fact that zircon was not detected by XRD-Rietveld analysis in the first two composites due to the thermal dissociation during processing. In the other materials the three phases (Z, B and M) were always observed.

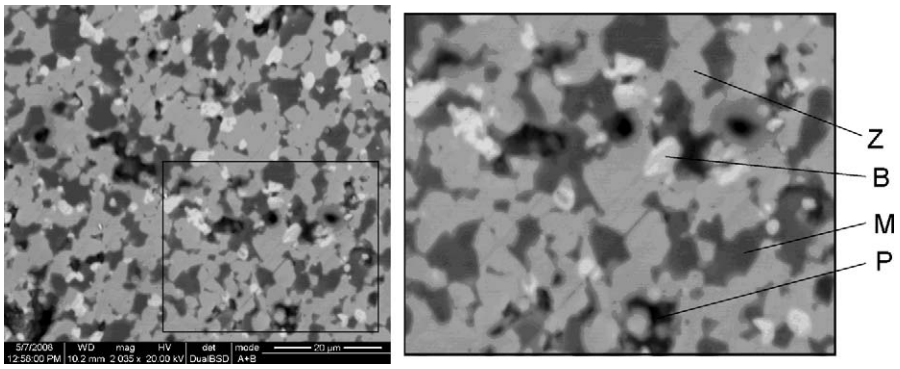

Fig. 7. SEM micrograph of the MZZ75 material. Example of the C type microstructure.

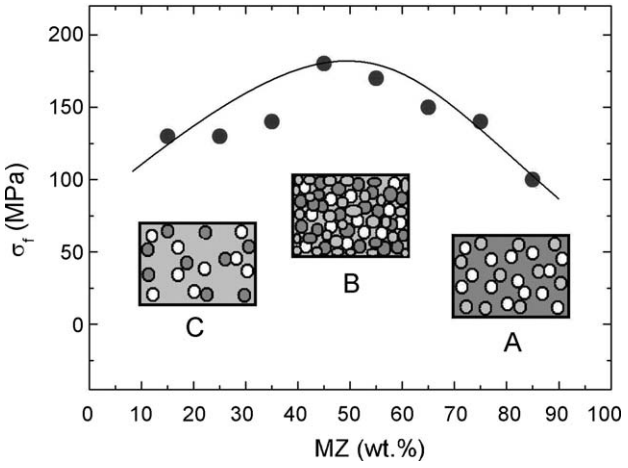

Fig. 8. Flexural strength as a function of the composition of the composites and the microstructure.

Microstructure configurations of the composites were grouped in three categories and labeled A, B and C. In Fig. 8 a schematic figure of the matrix configuration of the microstructure are shown for these groups:

A. The microstructure configuration of composites MZZ15–MZZ35 reveled a mullite matrix with well dispersed zirconia grains (2–5 μm) (corresponds to SEM micrograph in Fig. 5).
B. For MZZ45 and MZZ55 the microstructure configuration is not well defined and it is not possible to establish a continuous phase that acts as the matrix one (corresponds to SEM micrograph in Fig. 6).
C. Finally a zircon matrix configuration appears for high zircon content composites (MZZ65–MZZ85) the zircon grains present a 5–10 μm size with dispersed mullite (3–7 μm) and zirconia (2–4 μm) grains. In these materials zirconia grains are never surrounded only by mullite. They are always at the zircon–mullite interface (corresponds to SEM micrograph in Fig. 7).

3.4. Flexural strength (σ_f)

Flexural strength (σ_f) was evaluated by the 3-point bend test of the square section bars. The MZZ45 composite presented the higher strength. In Fig. 8 the values of the flexural strength of the different composites are shown as function of initial composition and correlated with material microstructure. Materials with no clear ceramic continuous phase (B) had the higher mechanical strength than materials with zircon (C) matrix or mullite (A) matrix. At low proportions the addition of zirconia grains dispersed in the ceramics (zircon) matrix increases the mechanical strength. To a small extent zircon addition also increases the flexural strength of mullite zirconia materials.

The values are slightly lower than those given in the literature for pure mullite (254 MPa) [6], pure zircon (150–320 MPa for various products fabricated at 1600 °C [8–11]) and 170–150 MPa for a zircon–mullite composite material (mullite ≈ 14 wt%) [14,16]. The difference may be explained by the residual porosity, microcracks resulting from the zirconia transformation during cooling, the presence of a non-crystalline phase, and the processing condition used.

3.5. Elastic modulus (E_0)

The impulse excitation technique was used to evaluate the elastic modulus. The results obtained by this method are reliable and results are comparable with those obtained by other methods such as 3- and 4-point bending methods or indentation techniques [28].

The experimental elastic modulus of the composites as a function of the initial proportion of MZ powder are shown in Fig. 9. The values obtained are slightly lower than those of pure zircon, pure zirconia and pure mullite ceramics (244 GPa, ≈200 GPa and 204 GPa respectively) [14].

The residual porosity of the composites was probably the main cause of the low measured modulus in comparison with the two single component materials.

Also in Fig. 9, a theoretical elastic modulus estimation (E_{teo}) is plotted against the amount of mullite–zirconia in the composition. Both elastic modulus the experimental and the theoretical one, decreased almost linearly with the increasing mullite content. This behavior is clearly shown in Fig. 9. The fitted straight lines follow the next equations (Eqs. (6) and (7)):

$$E_{teo} = 243.9 - 0.52\,MZ \quad (6)$$

$$E_0 = 233.5 - 1.08\,MZ \quad (7)$$

where MZ is the mullite–zirconia powder wt% incorporated in the composite and E_{teo} and E are the values of the theoretical and experimental elastic modulus in GPa, respectively.

Since the values of E of the three independent phases are comparable a gradual reduction on E may be interpreted as continuous change of the microstructure [29], for example as the appearance of microcracks due to the presence of the zirconia grains. The higher slope (absolute value) of the

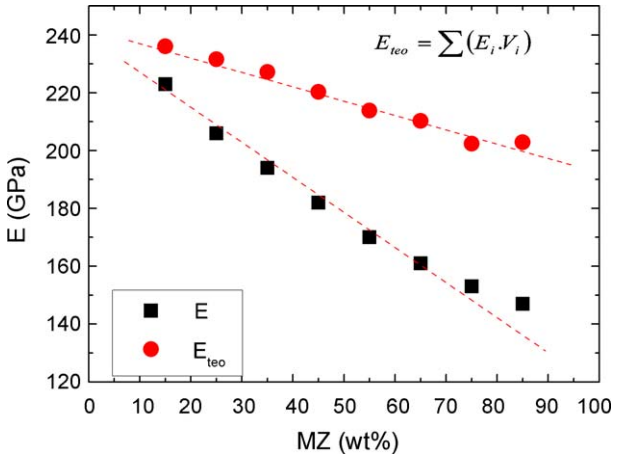

Fig. 9. Theoretical and experimental elastic modulus of the materials as a function of the initial composition.

experimental equation shows that the experimental change is higher than the change expected only taking into account the phase content of each phase.

In the final composite zirconia comes from both: the raw materials (MZ) and also from the thermal dissociation of the $ZrSiO_4$. In a similar group of materials [16] the higher decrease in the elastic modulus was attributed to this new ZrO_2 formed during sintering. Perhaps in this group of materials the higher content of zirconia also explains the higher decrease in E. This is linked to microcracks developed by the martensitic transformation of the zirconia during the processing (cooling). The thermal expansion mismatch between zirconia ($\alpha \approx 10 \times 10^{-6}\,^{\circ}C^{-1}$) and mullite and zircon ($\alpha \approx 4.5 \times 10^{-6}\,^{\circ}C^{-1}$ and $\alpha \approx 5.0 \times 10^{-6}\,^{\circ}C^{-1}$, respectively) might cause the development of microcracks during the processing of the composite materials. Both kinds of microcracks diminish the value of the elastic modulus of the final ceramic.

3.6. Fracture toughness (K_{IC}) and initiation fracture energy (γ_{NBT})

Many methods are currently used to measure the fracture toughness of ceramics materials. The NBT method is simple and inexpensive and has been successfully used in previous reports [16,25,26].

Together, fracture toughness (K_{IC}) and initiation fracture energy (γ_{NBT}) are plotted against the initial composition in Fig. 10, at first glance the values of fracture toughness (K_{IC}) and the fracture initiation energy (γ_{NBT}) are similar to the ones found in the literature for these materials [14,16]. Clearly both properties had been improved by the addition of mullite zirconia powder to the composite formula, moreover both increased linearly with of the mullite–zirconia (MZ) wt% incorporated. These behaviors are represented by Eqs. (8) and (9) respectively showing that the initial composition is a satisfactory processing variable for designing this kind of materials.

$$K_{IC} = 1.68 + 0.0125\,MZ \tag{8}$$

$$\gamma_{NBT} = 3.53 + 0.247\,MZ \tag{9}$$

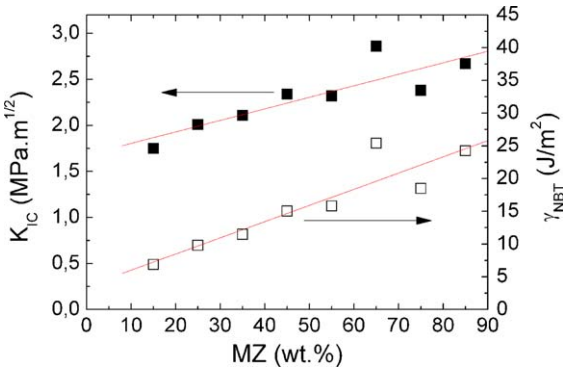

Fig. 10. Toughness (K_{IC}) and initiation fracture energy (γ_{NBT}) of the materials as a function of the initial composition.

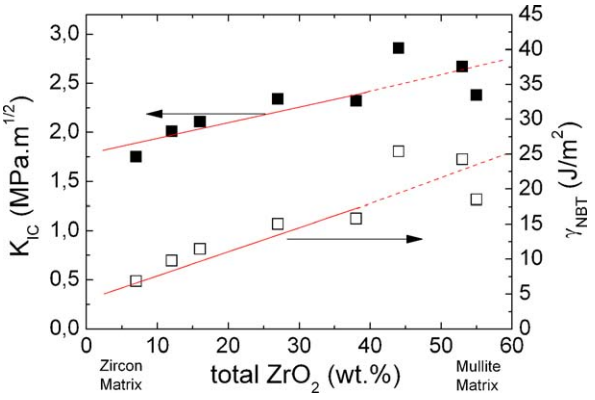

Fig. 11. Toughness (K_{IC}) and initiation fracture energy (γ_{NBT}) of the materials as a function of the total amount of zirconia.

4. Toughening

Significant toughening can be obtained by incorporating zirconia particles (ZrO_2) in a ceramic matrix. Different mechanisms are involved in the toughening: stress-induced transformation, microcraking, crack bowing and crack deflection. In all cases, the operative toughening mechanism depends on such variables as matrix stiffness, zirconia particle size, chemical composition, temperature and strength [30–32].

In Fig. 11, K_{IC} and γ_{NBT} are plotted against the amount of total ZrO_2 wt% (evaluates by the Rietveld method) showing that zirconia is involved in some of the mechanisms described above. As mentioned, zirconia comes from one of the raw materials (MZ) and from the thermal dissociation of the other raw material (zircon). Linear correlations were found in both fracture parameters, which follow correspondingly Eqs. (10) and (11), where Z is the total zirconia (m-ZrO_2 + t-ZrO_2) in the composite evaluated by the Rietveld method on weight basis.

$$K_{IC} = 1.81 + 0.0158Z \tag{10}$$

$$\gamma_{NBT} = 5.99 + 0.310Z \tag{11}$$

At higher ZrO_2 content the values are more dispersed but the increase is still clear. In the last values of the series (MZZ15 and MZZ25) a decrease is observed, perhaps because the microcracks concentration is so high that they are interconnected and led to a decrease in the toughness.

Finally zirconia free zircon–mullite materials are difficult to obtain [14,16] because of the mentioned the thermal dissociation of zircon which occurs even below 1400 °C depending on the impurities present that occurs during the thermal treatment during the processing. However, the toughness and initiation surface energy, by these equations, can be estimated (K_{IC} = 1.806 MPa $m^{1/2}$ and γ_{NBT} = 5.991 J/m^2) for a binary composite material with 45 wt% of mullite and 55 wt% of zircon.

5. Conclusions

Mullite–zirconia–zircon composites with different microstructures were processed from binary mixtures of zircon and mullite–zirconia powders.

In all the cases the microstructure dimension is comparable to the mean diameter of the starting powders.

Thermal dissociation of zircon was found during the processing (1600 °C for 2 h). Especially when it was in low proportions. The presence of mullite–zirconia grains promoted this decomposition process. The zirconia present in the final materials was almost all monoclinic (99–98%). No crystalline silica was detected (XRD); hence it is correct to assume that it is in the glassy phase.

SEM examination confirmed a progressive change in the microstructure from mullite matrix with zirconia and zircon dispersed grains to a zircon matrix with mullite and zirconia as discrete phases. The microstructure configuration is well represented by the phase volume content estimated by the Rietveld method.

Mechanical and fracture properties of the composites were measured. While the flexural strength was related to the microstructure configuration, the other properties (E, K_{IC} and γ_{NBT}) presented clear linear correlation with the composites composition.

Materials with equal proportion of the three phases, where no continuous matrix can be defined presented the higher flexural strength (MZZ45).This maximum in the mechanical strength could indicate that the zirconia content in this particular composite is optimum and that over this proportion the influence of the microcracks starts to be negative.

The elastic modulus decreased with the increase of the proportion of mullite–zirconia. Moreover this decrease was higher than the predicted by from the rule of mixtures, probably due to the presence of microcracks resulting from the ZrO_2 transformation during the cooling cycle of the processing thermal treatment.

The fracture toughness and the initiation surface energy were increased by the increase of the MZ content, which increased with zirconia content and the zircon dissociation.

The composites with higher amounts of zirconia had higher fracture toughness; this could be linked to several toughening mechanisms. The induced microcracks promote the fracture resistance of these composites. But there is insignificant amount of t-ZrO_2 in these composites and no transformation toughening is expected.

References

[1] Y. Shi, X. Huang, D. Yan, Fabrication of hot-pressed zircon ceramics: mechanical properties and microstructure, Ceram. Int. 23 (1997) 457–462.

[2] A. Everett, T. Thomas, T. Weichert, Trends in usage in glass industry, Proc. UNITECR (1989) 730–760.

[3] J. Mori, N. Watanbe, M. Yoshimura, Y. Oguchi, T. Kawakami, A. Matsuo, Materials design of monolithic refractories for steel ladle, Proc. UNITECR (1989) 541–553.

[4] L.B. Garrido, E.F. Aglietti, Zircon based ceramics by colloidal processing, Ceram. Int. 5 (2001) 491–499.

[5] R. Torrecillas, J. Calderon, J. Moya, M. Reece, C. Davies, C. Olagnond, G. Fantozzi, Suitability of mullite for high temperature applications, J. Eur. Ceram. Soc. 19 (1999) 2519–2527.

[6] M. Hamidouche, N. Bouaouadja, C. Olagnon, G. Fantozzi, Thermal shock behavior of mullite ceramic, Ceram. Int. 29 (2003) 599–609.

[7] H. Schneider, J. Schreuer, B. Hildmann, Structure and properties of mullite—a review, J. Eur. Ceram. Soc. 28 (2008) 329–344.

[8] C. Veytizou, J. Guinson, Y. Jorand, Preparation of zircon bodies from amorphous precursors powders synthesized by sol–gel processing, J. Eur. Ceram. Soc. 22 (2002) 2901–2909.

[9] Y. Shi, X. Huang, D. Yan, TEM and SEM characterization of hot-pressed zircon ceramics, Mater. Lett. 23 (1995) 247–252.

[10] R. Moreno, J. Moya, J. Requena, Slip casting of zircon by using an organic surfactant, Ceram. Inter. 17 (1991) 37–40.

[11] T. Mori, H. Yamamura, H. Kobayashi, T. Mitamura, preparation of high-purity $ZrSiO_4$ using sol–gel processing and mechanical properties of the sintered body, J. Am. Ceram. Soc. 75 (9) (1990) 2420–2426.

[12] R. Singh, SiC fibre-reinforced zircon composites, J. Am. Ceram. Soc. Bull. 70 (I) (1991) 555–556.

[13] Y. Shi, X. Huang, D. Yan, Toughening of hot-pressed $ZrSiO_4$ ceramics by addition of y-TZP, Mater. Lett. 35 (3) (1998) 161–165.

[14] M. Hamidouche, N. Bouaouadja, R. Torrecillas, G. Fantozzi, Thermo-mechanical behavior of a zircon–mullite composite, Ceram. Int. 33 (4) (2007) 655–662.

[15] N.M. Rendtorff, L.B. Garrido, E.F. Aglietti, Effect of the addition of mullite–zirconia to the thermal shock behavior of zircon materials, Mater. Sci. Eng. A 498 (1–2) (2008) 208–215.

[16] N.M. Rendtorff, L.B. Garrido, E.F. Aglietti, Mechanical and fracture properties of zircon–mullite composites obtained by direct sintering, Ceram. Int. 35 (7) (2009) 2907–2913.

[17] P. Descamps, S. Sakaguchi, M. Poorteman, F. Cambier, High temperature characterization of reaction sintered mullite–zirconia composites, J. Am. Ceram. Soc. 10 (1991) 2476–2481.

[18] N. Claussen, J. Jahn, Mechanical properties of sintered in situ reacted mullite–zirconia composites, J. Am. Ceram. Soc. (Note) 3–4 (1980) 228–229.

[19] K. Das, S.K. Das, B. Mukherjee, G. Barnerjee, Microstructural and mechanical properties of reaction sintered mullite–zirconia composites with magnesia as additive, Interceramics 5 (1998) 304–313.

[20] F. Temoche, L.B. Garrido, E.F. Aglietti, Processing of mullite–zirconia grains for slip cast ceramics, Ceram. Int. 31 (2005) 917–922.

[21] N.M. Rendtorff, L.B. Garrido, E.F. Aglietti, Mullite–zirconia–zircon composites: properties and thermal shock resistance, Ceram. Int. 35 (2) (2009) 779–786.

[22] D.L. Bish, J.E. Post, Quantitative mineralogical analysis using the Rietveld full-pattern fitting method, Am. Min. 78 (1993) 932–940.

[23] C. Rodriguez, FullProf, a program for Rietveld refinement and pattern matching analysis, in: Abstracts of the Satellite Meeting on Powder Diffraction of the IUCr, Toulouse, France, (1990), p. 12.

[24] H.M. Rietveld, A profile refinement method for nuclear and magnetic structures, J. Appl. Crystallogr. 2 (1969) 65–71.

[25] V. Pandolfelli, V. Salvini, Influence of mullitte–zirconia aggregate addition on the thermomechanical properties of high-alumina refractories, Ann. UNITECR (1993) 282–291.

[26] H. Harmuth, E. Tsechegg, Fracture mechanical characterization of ordinary ceramic refractory materials, Veitsch-Radex-Rundschau 1–2 (1994) 465–542.

[27] A. Kaiser, M. Lobert, R. Telle, Thermal stability of zircon ($ZrSiO_4$), J. Eur. Ceram. Soc. 28 (2008) 2199–2211.

[28] R.C. Bradt, Problems and possibilities with cracks in ceramics, Science of Ceramics, vol. 11, Gotemborg, Sweden, 1981.

[29] M. Radovic, E. Lara-Curzio, L. Riester, Comparison of different experimental techniques for determination of elastic properties of solids, Mater. Sci. Eng. A 368 (March (1–2)) (2004) 56–70.

[30] X. Jin, Martensitic transformation in zirconia containing ceramics and its applications, Curr. Opin. Solid State Mater. Sci. 9 (6) (2005) 313–318.

[31] P.M. Kelly, L.R. Francis Rose, The martensitic transformation in ceramics—its role in transformation toughening, Prog. Mater. Sci. 47 (5) (2002) 463–557.

[32] N. Claussen, J. Jahn, Mechanical properties of sintered in situ reacted mullite–zirconia composites, J. Am. Ceram. Soc. 63 (34) (1980) 228–229.